Computational models for design of concrete segments with symmetrical reinforcement bars under the action of bending moments and axial forces

† Li Shouju [1]*, Shangguan Zichang[2], and Feng Ying [1]

[1] State Key Laboratory of Structural Analysis for Industrial Equipment, Dalian University of Technology, Dalian 116024, China.

[2] Institute of Marine and Civil Engineering, Dalian Ocean University, Dalian, 116023, China

*Presenting author: lishouju@dlut.edu.cn

†Corresponding author: lishouju@dlut.edu.cn

Abstract

Shield-driven tunnels are widely adopted in the development of underground spaces for transportation and utility networks in soft soils. Numerical modeling has now become an important element in the design of underground excavations in soils and rocks. Numerical analysis can provide realistic representation of the field conditions taking into account key elements of the excavation such as the geomechanical characteristics of the ground and the in situ stress condition. In order to solve the problems of section design and verification of concrete segments, the computational models are proposed for designs of concrete segments with symmetrical reinforcement bars under the action of bending moments and axial forces. Based on the constitutive model of steel bars and similarity criterions of strains in beam section, the analytical expression of stress on reinforcement bars located in compressive region is derived. Influences of axial forces on the ultimate bearing bending moment of segments and the area of reinforcement bars in tension region are discussed through analyzing two practical underground tunnels with concrete segment linings. The investigation shows that the depth of compressive region increases ith increasing axial force on segment. The ultimate bearing bending moment of concrete segment increases with increasing axial force on segment when area of reinforcement bars is constant.

Keywords: Concrete segment, Section design and verification, Bending moment, Axial force, Computational model.

Introduction

Reinforced concrete segments are widely used in Metro tunnels, hydraulic tunnels and mining tunnels. The optimal design and analysis of ultimate bearing performance for concrete segments refer to safety and economic problems of underground structures. Especially with commonly using shield machine in underground engineering, the investigations about ultimate bearing performance for concrete segments have received general attentions in domestic and overseas. Jiang studied influences of hybrid tendons, load locations and joint numbers to flexural strength of fully segmental beams. For comparison purpose, a monolithic beam with hybrid tendons was also tested. The deflections, ultimate loads, stresses of prestressing strands and failure modes were investigated. At the ultimate stage, the stresses of all tendons are greater than 1500 MPa[1]. Caratelli performed full-scale tests on both traditional reinforced concrete and fiber reinforced elements. In particular, bending tests were carried out in order to compare the behaviour of the segments under flexural actions, while point load tests were developed with the aim of simulating the thrustforce induced by the Tunnel Boring Machine, and then the effect of load concentration and splitting phenomena[2]. Yan presented a comprehensive experimental study on the comparative behaviour of the reinforced concrete and the hybrid fibre reinforced concrete shield TBM tunnel lining segments exposed to fire. The tests were conducted using a newly developed test facility, which is capable of accommodating different mechanical loading and boundary conditions under different fire scenarios[3]. Shalabi proposed lining structure which was made of bolted and double gasketed precast concrete segment lining with convex to convex longitudinal joint surfaces. Lining evaluation included the sealant performance of different gasket materials under water pressure less than 90 psi. Testing program was designed to evaluate the longitudinal joint and T-joint sealant behavior under static and dynamic loading using large scale concrete segments[4]. Nehdi investigated the mechanical performance of Ultra-high performance fiber-reinforced concrete tunnel lining segments. Flexural and edge-point load tests were conducted on 1/3-scale tunnel lining segments to evaluate its bending and thrust load resistance[5]. Zhang proposed a method based on the moment-force interaction and the effect of bolt pockets. The method considered that the load corresponding to the appearance of the first crack is the load of bond cracking, and assumed that the K-segment is a column which is subjected to axial loading and biaxial bending. Analytical results were compared with experimental values obtained from four reinforced-concrete K-segments[6].Amau studied the phenomena associated to coupling effects, determines the main involved parameters and analyzes their influence on a real lining structural response by means of a 3D numerical model. The comparison with the usual plane models currently employed in linings designs provide significant conclusions about the coupling effects implications and the conditions in which become more relevant[7].Analysis from Ye on the effective ratio of the transverse bending rigidity values under different load levels with different bolt pre-tightening forces and different assembly modes shows that value of the stagger-jointed segmental ring is obviously lager than that of the straight-jointed segmental ring, and that difference decrease gradually with the load increasing[8].Analysis from Moller shown that installation procedures are most important to be considered in order to arrive at proper predictions for tunneling settlements, horizontal deformations and lining forces. For the installation of closed face shield tunneling a novel simulation method is presented, named the grout pressure method. It is shown that the grout pressure method yields the best predictions for both ground movements and structural forces[9]. Do proposed the influence of joint rotational stiffness, the reduction in joint rotation stiffness under the negative bending moment, the lateral earth pressure factor and Young modulus of ground surrounding the tunnel should not be neglected. On the other hand, the results have also shown an insignificant influence of the axial and radial stiffness of the joints on segmental tunnel lining behavior[10]. The aim of the paper is to propose the relationship between the ultimate bending moment of concrete segment and axial force, analyze stress state of reinforced bars in compressive zone, investigate the worst loading combination between bending moment and axial force, and further develop computing models for evaluating ultimate bearing performances of concrete segments.

Current computing models for ultimate bearing performances of concrete segments

The concrete segments are idealized as column with loading of eccentric force N. Based on Code for design of concrete structures, assume that the deformed bars on compressive zone and tensile zone are yielded. An equivalent rectangular stress distribution is simplified with little loss in accuracy, as shown in Fig. 1

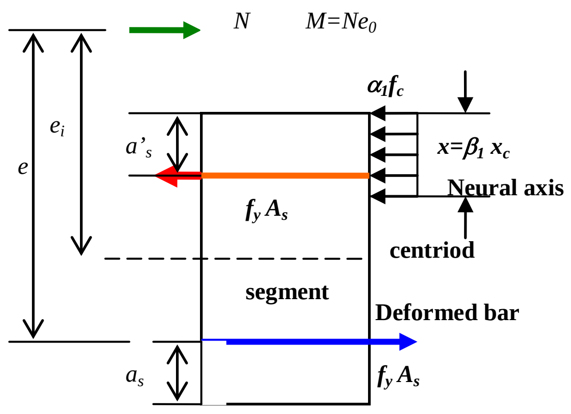

Figure 1. Idealized computational models for concrete segments with symmetrical reinforcement bars

It is assumed that the axial force, concrete grade and area of deformed bar are known. Based on the balance of forces acting on the section, as shown in Fig. 1, it is given by

$$N = \alpha_1 f_c bx \tag{1}$$

Where N is axial force,a_1 is stress coefficient, x is depth to neural axis, b is width of segment, f_c is compressive strength of concrete. The depth of neural axis is expressed as follows

$$x = \frac{N}{\alpha_1 f_c b} \tag{2}$$

The ultimate bearing bending moment of concrete segment is derived as

$$\begin{aligned} M_u &= Ne_0 \\ &= \alpha_1 f_c \frac{N}{\alpha_1 f_c b} b(h_0 - 0.5\frac{N}{\alpha_1 f_c b}) \\ &+(h_0 - a_s) f_y A_s - N(h/2 - a_s + e_a) \end{aligned} \tag{3}$$

Where e_0 is a distance (original eccentricity) from the centroid of deformed bar to axial force, M_u is ultimate bending moment, a_s is vertical distance from the joint point of all longitudinal tension bars to the cross section of the cross section, h is section height, h_0 is section effective height, h_0=h-a_s, A_s is reinforced area, f_y is tensile strength of reinforcement.

$$e_0 = e_i - e_a \tag{4}$$

Where e_i is a distance from the centroid of section to axial force accounting for adding eccentricity, as shown in Fig. 1. e_a is a adding eccentricity.

$$e_i = e - h/2 + a_s \tag{5}$$

$$e = \frac{\alpha_1 f_c xb(h_0 - 0.5x) + (h_0 - a_s) f_y A_s}{N} \tag{6}$$

Where e is a distance from the centroid of deformed bar in tensile zone to axial force.
Based on Code for design of concrete structures, evaluate the segment is in a state of small eccentricity or large eccentricity according to following formulas

$$N_{ub} = \alpha_1 f_c bx_b \tag{7}$$

Where N_{ub} is ultimate compressive force of segment under boundary condition, x_b is boundary depth to neural axis. If $N<N_{ub}$, then segment is in a state of large eccentricity; otherwise in a state of small eccentricity.

$$x_b = \xi_b h_0 \tag{8}$$

Where ζ_b is relative boundary depth to neural axis.

$$\xi_b = \frac{\beta_1}{1 + \frac{f_y}{E_s \varepsilon_{cu}}} \tag{9}$$

Where E_s is elastic modulus of reinforcement, ε_{cu} is ultimate strain of concrete, ε_{cu}=0.0033. The calculating steps for ultimate bearing performance of concrete segment are listed as: Step 1) Evaluate the segment is in a state of small eccentricity or large eccentricity according to equation (7); Step 2) Calculate depth to neural axis according to equation (2); Step 3) Calculate a distance (eccentricity) from the centroid of deformed bar to axial force according to equation (4), (5) and (6); Step4) Calculate ultimate bearing bending moment of concrete segment according to equation (3).

New computing models for ultimate bearing performances of concrete segments

Accounting for the specifics of concrete segments in Metro tunnels, such as higher concrete grade, and section height of segments far less than section width of segments, the depth to neural axis is smaller and the stress of deformed bars in compressive zone is less than yield limit, and even the stress of deformed bars in compressive zone is in tensile state. So, based on current computing models, the practical stress of deformed bars in compressive zone is different from model solutions.

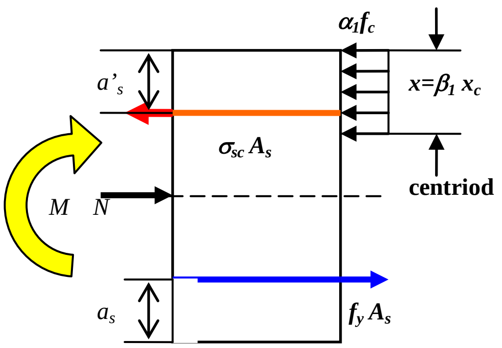

Fig. 2 Force and bending moment balances for column with eccentric compressive loading

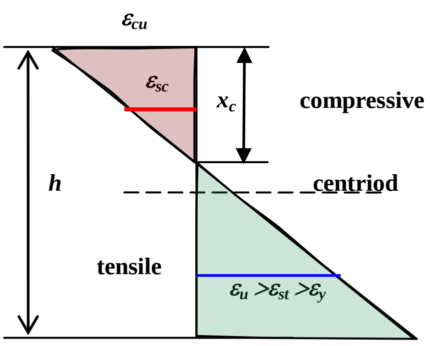

Fig. 3 Simplified strain distributions on concrete segment

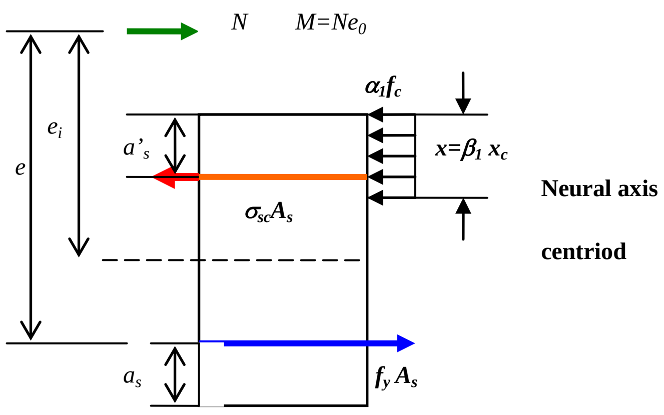

Fig. 4 Idealized computational models for concrete segments with symmetrical reinforcement bars and eccentric compressive loading

Based on force balance, as shown in Fig. 2 and 4, it is derived as

$$N = \alpha_1 f_c bx + \sigma_{sc} A_s - f_y A_s \tag{10}$$

Where σ_{sc} is compressive stress of reinforcement. The depth to neural axis is expressed as

$$x = \frac{N - \sigma_{sc} A_s + f_y A_s}{\alpha_1 f_c b} \tag{11}$$

Assume that the stress of deformed bar in compressive zone is less than yield limit, the relation between stress and strain for deformed bars is given by

$$\sigma_{sc} = \varepsilon_{sc} E_s \tag{12}$$

Under the action of axial force with an eccentricity *e*, and based on plane deformation assumption, as shown in Fig. 3, the relation between strain of deformed bars in compressive zone and ultimate strain of concrete is given by

$$\frac{\varepsilon_{sc}}{\varepsilon_{cu}} = \frac{x_c - a_s}{x_c} = (1 - \frac{\beta_1 a_s}{x}) \tag{13}$$

Were β_1 is a factor that is a function of the strength of the concrete, a_s is the distance from the center of tensile bars to inter surface of segment, as shown in Fig.4. x_c is distance from the outer compressive fiber to neural axis, and x is depth of neural axis for simplified equivalent rectangular. ε_{cu} is ultimate strain of concrete, ε_{cu}=0.0033. If ε_{sc}>0, then the stress of deformed bars in compressive zone is in compressive state; otherwise in tensile state.

$$\varepsilon_{sc} = \varepsilon_{cu} (1 - \frac{\beta_1 a_s}{x}) \tag{14}$$

Substitute equation (14) into equation(12), it is obtained

$$\sigma_{sc} = E_s \varepsilon_{cu} (\frac{x - \beta_1 a_s}{x}) \tag{15}$$

Substitute equation (15) into equation (11), it is obtained

$$x = \frac{N - E_s \varepsilon_{cu} (\frac{x - \beta_1 a_s}{x}) A_s + f_y A_s}{\alpha_1 f_c b} \tag{16}$$

$$\alpha_1 f_c b x^2 - (N + f_y A_s + E_s \varepsilon_{cu} A_s) x - E_s \varepsilon_{cu} A_s \beta_1 a_s = 0 \tag{17}$$

The depth to neural axis is solved by equation (17), and then the stress of deformed bars in compressive zone is obtained by equation (15). Based on the balance principle of force moment, as shown in Fig.3, it is obtained

$$Ne = \alpha_1 f_c x b (h_0 - 0.5x) + (h_0 - a_s) \sigma_{sc} A_s \tag{18}$$

$$e = \frac{\alpha_1 f_c x b (h_0 - 0.5x) + (h_0 - a_s) \sigma_{sc} A_s}{N} \tag{19}$$

$$\begin{aligned} e_0 &= e - h/2 + a_s - e_a \\ &= \frac{\alpha_1 f_c x b (h_0 - 0.5x) + (h_0 - a_s) \sigma_{sc} A_s}{N} - (h/2 - a_s + e_a) \end{aligned} \tag{20}$$

The ultimate bearing bending moment of concrete segment is derived as

$$\begin{aligned} M_u &= N e_0 \\ &= \alpha_1 f_c x b (h_0 - 0.5x) + (h_0 - a_s) \sigma_{sc} A_s - N(h/2 - a_s) \end{aligned} \tag{21}$$

The calculating steps of proposed new models for ultimate bearing performance of concrete segment are listed as: Step 1) Evaluate the segment is in a state of small eccentricity or large eccentricity according to equation (7); Step 2) Calculate depth to neural axis according to equation (17); Step 3) Calculate the stress of deformed bars in compressive zone according to equation (15); Step 4) Calculate a distance (eccentricity) from the centroid of deformed bar to axial force according to equation (20); Step5) Calculate ultimate bearing bending moment of concrete segment according to equation (21).

Case study for two Metro tunnels

In order to investigate the differences between current models and new proposed models, two practical Metro tunnels with concrete segment lining are studied. The stress distribution in deformed bars and ultimate bending moment are calculated respectively. The drawbacks of current models are discussed in detail. The first practical engineering example is Beijing Metro tunnel[11]. The maximum embedded depth of tunnel is 10. 31m. The outer diameter of tunnel segment is 6.0m. The height of segment is 300mm. The width of segment is 1.2m. Concrete Grade is C50 with symmetrical reinforcement bars. The yield limit of bars is 300MPa. The area of deformed bars is

2514mm2 both for compressive zone and tensile zone, respectively. The distance from the center of tensile bars to inter surface of segment is as=40mm.

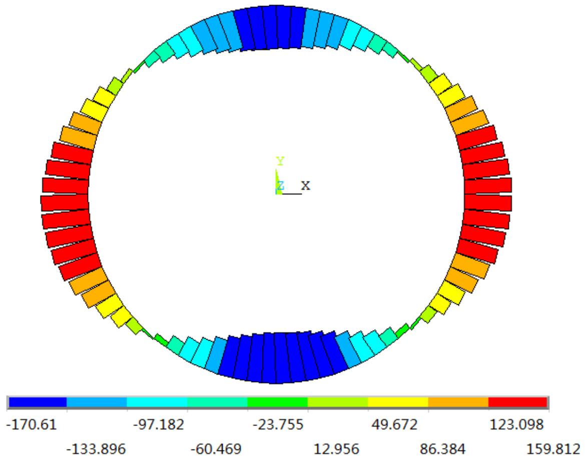

Fig. 5 Bending moment distributions on concrete segments (Unit: kNm, Beijing Metro tunnel)

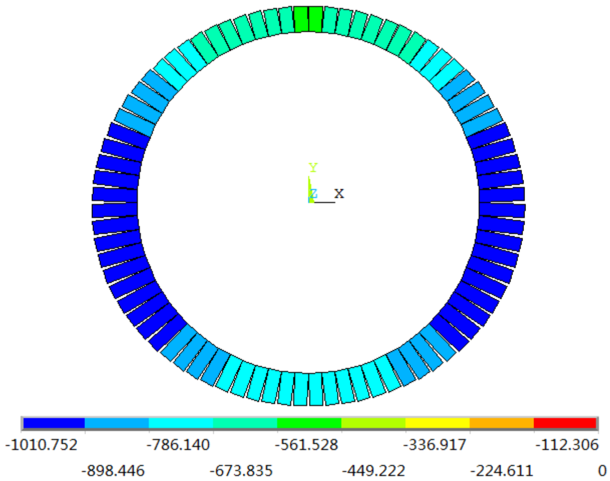

Fig. 6 Axial force distributions on concrete segments (Unit: kN, Beijing Metro tunnel)

Finite element method is used to compute the internal force distributions on segments for Beijing Metro tunnel , as shown in Fig. 6 and 7. It is obtained from Fig.6 and 7 that The maximum bending moment on segments is 160 kNm. The axial force on segments is in compressive state and varied from 400kN to1010kN. Variations of ultimate bending moment of segments versus axial force are listed in Table 1 and 2.

Table 1 Variation of ultimate bending moment of segments versus axial force (Current model, Beijing Metro tunnel)

Axial force /kN	400	500	600	700	800	900	1000
x/mm	14.4	18.1	21.6	25.25	28.8	32.5	36.1
$M_u/kN{\cdot}m$	215	226	237	248	258	268	278
σ_{sc} */MPa*	300	300	300	300	300	300	300

Table 2 Variation of ultimate bending moment of segments versus axial force (New proposed model, Beijing Metro tunnel)

Axial force /kN	400	500	600	700	800	900	1000
x/mm	35.6	37.0	38.6	40.2	41.9	43.6	45.5

M_u /kN·m	224	233	242	251	260	269	278
σ_{sc} /MPa	66	90	113	134	156	176	196

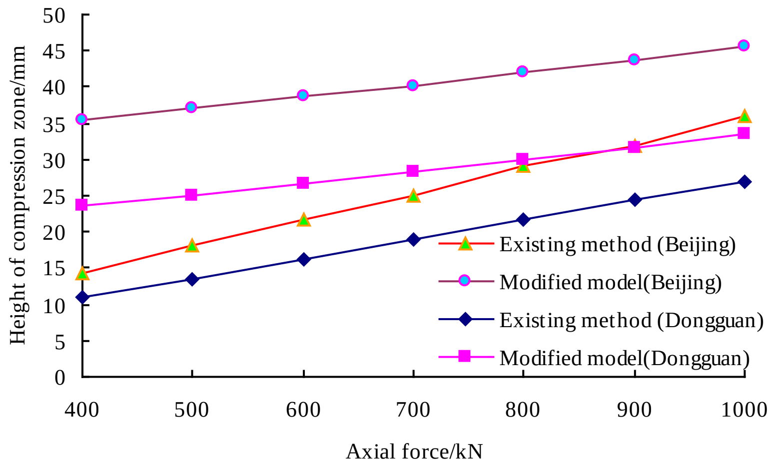

Fig. 7 Variation of compressive depth versus axial forces

It is found from Fig.7 that the compressive depth in concrete segment increases with increasing axial force, and the compressive depth in new proposed model is larger than one in current model.

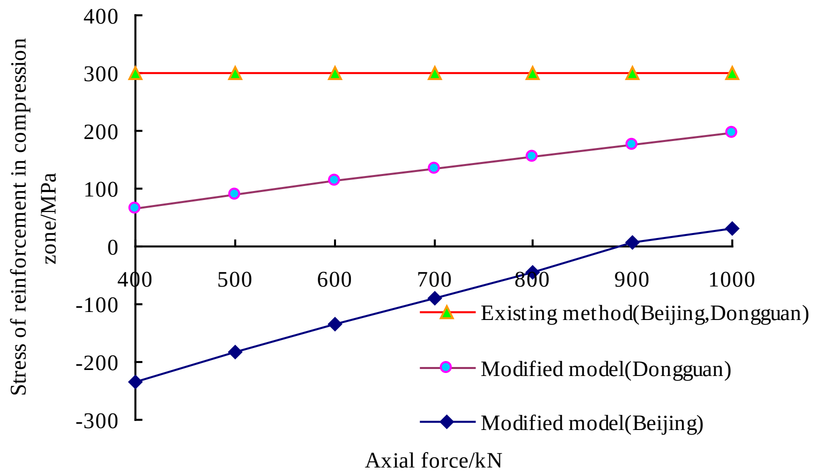

Fig. 8 Variation of stress of reinforced bars in compressive zone versus axial forces

It is found from Fig.8 that the stress of reinforced bars in compressive zone increases with increasing axial force. The stress of reinforced bars in compressive zone is less than yield strength, especially for Dongguan tunnel, the stress of reinforced bars in compressive zone is in tensile state.

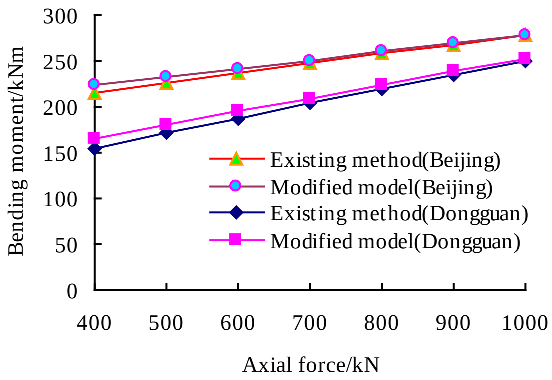

Fig. 9 Variation of ultimate bending moment of segments versus axial force

It is observed from Fig. 9 that the ultimate bending moments of segments for both current and new proposed models are nearly same even if the compressive depths and stresses of reinforced bars in compressive zone for two models are different. The second practical engineering example is Dongguan-Huizhou tunnel under water[12]. The maximum embedded depth of tunnel is 16. 2m. The maximum water depth is 16. 2m. The outer diameter of tunnel segment is 8.5m. The height of segments is 400mm. The width of segments is 1.6m. Concrete Grade is C50 with symmetrical reinforcement bars. The yield limit of bars is 300MPa. The area of deformed bars is 882mm2 both for compressive zone and tensile zone, respectively. The distance from the center of tensile bars to inter surface of segment is as=40mm. The maximum bending moment acting on segments is 90kNm. The maximum axial force is 100kN. Variations of ultimate bending moments of segments versus axial force are listed in Table 3 and 4, respectively.

Table 3 Variation of ultimate bending moment of segments versus axial force (Current model, Dongguan tunnel)

Axial force /kN	**400**	**500**	**600**	**700**	**800**	**900**	**1000**
x/mm	10.8	13.5	16.2	18.9	21.6	24.4	27.0
M_u//kN·m	154	171	188	204	220	235	253
σ_{sc} /MPa	300	300	300	300	300	300	300

Table 4 Variation of ultimate bending moment of segments versus axial force (New proposed model, Dongguan tunnel)

Axial force /kN	400	500	600	700	800	900	1000
x/mm	23.6	25.0	26.6	28.2	30.0	31.6	33.5
M_u /kN·m	165	180	195	209	224	239	251
σ_{sc} /MPa	-235	-182	-134	-88	-46	7	30

Note: Negative represents deformed bars in tensile state.

Conclusions

1) The investigation validates that the stress of reinforced bars in compressive zone increases with increasing axial force. The compressive depth in concrete segment is far less than 2as, so the stress of reinforced bars in compressive zone is less than yield strength. Especially for Dongguan tunnel, the stress of reinforced bars in compressive zone is in tensile state.

2) Two practical Metro tunnels with concrete segment lining are computed by using two different models. The results show that the compressive depth in concrete segment increases with increasing axial force, and the compressive depth in new proposed model is larger than one in current model. The worst loading combination is maximum bending moment with minimum axial force.
3) It is observed that the ultimate bending moments of segments for both current and new proposed models increase with increasing axial force, and are nearly same even if the compressive depths and stresses of reinforced bars in compressive zone for two models are obviously different. The proposed computing model can precisely calculate the stresses of reinforced bars in compressive zone.

Acknowledgments

The research described in this paper was financially supported by the National Key Basic Research and Development Program of China (Grant No. 2015CB057804), the National Natural Science Foundation of China (Grant No. 11572079) and Opening Foundation of State Key Laboratory of Structural Analysis for Industrial Equipment (Grant No. S14206).

References

[1] Jiang, H. B., Cao Q., Liu, A. R.. (2016) Flexural behavior of precast concrete segmental beams with hybrid tendons and dry joints. *Construction and Building Materials* **110**, 1-7.

[2] Caratelli, A., Meda, A., Rinaldi, Z.. (2011) Structural behaviour of precast tunnel segments in fiber reinforced concrete. *Tunneling and Underground Space Technology* **26**, 284-291.

[3] Yan, Z. G., Yi, S., He, H. Z.. (2015) Experimental investigation of reinforced concrete and hybrid fibre reinforced concrete shield tunnel segments subjected to elevated temperature. *Fire Safety Journal* **71**, 86-99.

[4] Shalabi, F., Cording, E., Paul, S.. (2012) Concrete segment tunnel lining sealant performance under earthquake loading. *Tunnelling and Underground Space Technology* **31**, 51-60.

[5] Nehdi, M., Abbas, S., Soliman, A.. (2015) Exploratory study of ultra-high performance fiber reinforced concrete tunnel lining segments with varying steel fiber lengths and dosages. *Engineering Structures* **101**, 733-742.

[6] Zhang, W. J., Koizumi, A..(2007) A study of the localized bearing capacity of reinforced concrete K-segment. *Tunnelling and Underground Space Technology* **22**, 467-473.

[7] Arnau, O., Molins, C.. (2013) Three dimensional structural response of segmental tunnel linings, *Engineering Structures* **44** , 210 -221.

[8] Ye, F., Gou, C. F., Sun, H. D.. (2014) Model test study on effective ratio of segment transverse bending rigidity of shield tunnel, *Tunnelling and Underground Space Technology* **41**, 193-205.

[9] Moller, S. C., Vermeer, P. A.. (2008) On numerical simulation of tunnel installation, *Tunneling and Underground Space Technology* **23**, 461-475.

[10] Anh, N., Do, D. D., Oreste, P.. (2013) 2D numerical investigation of segmental tunnel lining behavior. *Tunnelling and Underground Space Technology* **37** ,115-127.

[11] Chen, D..(2009) . Comparative analysis of designing methods of tunnel segments for Beijing Metro. *Railway Standard Design* **10**, 60-64.

[12] Hu, H., Zhang, L., Qiu, W. G.. (2012) Comparative analysis of three kinds of designing methods of tunnel segments and field experiment investigation. *Hydrogeology and Engineering Geology* **39**, 72-76.